

RESEARCH PAPER

## Comparative Effects of Orlistat and PEG-SPIONs on Fasting Glucose, Insulin, and Leptin in Obese Male Mice

Safa Abd al-karim Ramadan, Aswan Al-Abboodi \*, Zainab Abduljabbar Ridha Al-Ali

Department of Biology, College of Science, University of Misan, Maysan, Iraq

### ARTICLE INFO

**Article History:**

Received 11 April 2026

Accepted 26 June 2026

Published 01 July 2026

**Keywords:**

Adipokines

Fe<sub>3</sub>O<sub>4</sub> nanoparticles

Insulin

Insulin resistance

PEG-SPIONs

### ABSTRACT

Orlistat reduces dietary fat absorption, whereas PEG-coated superparamagnetic iron-oxide nanoparticles (PEG-SPIONs) have been reported to modulate adiposity and thermogenic pathways. Whether PEG-SPIONs can augment orlistat's metabolic effects in obesity remains uncertain. Seventy adult male mice were allocated to five groups (n=14 each group): control (A), obese untreated (B), orlistat (C), PEG-SPIONs (D), and orlistat+PEG-SPIONs (E). Treatments were given orally; subsets were sampled at 7 and 21 days. Fasting glucose, serum insulin, and leptin were measured and the fasting glucose was higher in all experimental groups than in controls (A), with the greatest elevation in obese mice (B). PEG-SPIONs (D) and the combination (E) showed lower glucose than obese mice (B), whereas orlistat alone (C) did not differ from B and was statistically comparable to D and E. Insulin concentrations did not differ among groups. For leptin, orlistat (C) and the combination (E) were higher than control (A) and PEG-SPIONs (D); control (A) and obese (B) did not differ, and B was comparable to C and E. PEG-SPIONs (D) were lower than obese (B) and orlistat (C/E) for leptin. In this model, PEG-SPIONs produced clearer improvements in fasting glycemia and a more favorable leptin profile than orlistat, without detectable changes in basal insulin. Co-administration with orlistat improved glucose versus obesity but did not surpass PEG-SPIONs alone and offered no advantage for leptin. These findings prioritize PEG-SPIONs as the main driver of benefit under the present regimen and motivate dose duration optimization and direct assessments of insulin sensitivity in future work.

### How to cite this article

Ramadan S., Al-Abboodi A., Al-Ali Z. Comparative Effects of Orlistat and PEG-SPIONs on Fasting Glucose, Insulin, and Leptin in Obese Male Mice. J Nanostruct, 2026; 16(3):3861-3868. DOI: 10.22052/JNS.2026.03.072

### INTRODUCTION

Obesity perturbs whole-body energy homeostasis and drives metabolic derangements that include insulin resistance, dysregulated glucose handling, and altered adipokine signaling. Expansion of white adipose depots elevates circulating free fatty acids (FFAs), attenuating insulin's antilipolytic action and diminishing glucose

uptake [1]. Oxidative stress further impairs insulin signaling and amplifies these defects [2]. Leptin, an adipocyte-derived hormone that links energy stores to appetite and expenditure, typically rises with adiposity, whereas central responsiveness to leptin declines so-called leptin resistance owing in part to limitations in transport and signaling at the blood-brain barrier [3, 4].

\* Corresponding Author Email: [aswan.abboodi@uomisan.edu.iq](mailto:aswan.abboodi@uomisan.edu.iq)



This work is licensed under the Creative Commons Attribution 4.0 International License.

To view a copy of this license, visit <http://creativecommons.org/licenses/by/4.0/>.

Orlistat, a gastrointestinal lipase inhibitor, reduces dietary fat absorption and can mitigate weight gain and improve indices of insulin resistance and oxidative stress in rodent models [5]. However, the magnitude of benefit varies with dose, exposure time, and dietary background. In parallel, superparamagnetic iron-oxide nanoparticles (SPIONs; Fe<sub>3</sub>O<sub>4</sub>) especially when polyethylene-glycol (PEG)-coated to enhance dispersion and biocompatibility have emerged as a materials-driven strategy to influence adiposity. Several studies indicate that iron-oxide nanoparticles can promote browning of white adipose tissue and augment brown adipose activity, shifting energy balance away from storage and improving glycemic control [6, 7]. At the nanoscale, surface chemistry critically determines biointerface behavior PEGylation and related surface modifications modulate protein adsorption, cell material interactions, and colloidal stability [8- 15]. A recent study shows that aligning surface chemistry, microtopography, and release kinetics with the local tissue milieu governs adhesion, fouling, and therapeutic performance principles that likewise motivate PEG-based surface engineering of SPIONs for stable dispersion and a favorable biointerface [16- 18].

The broad biomedical footprint of nanomaterials including antimicrobial applications of nanoparticle effects within biofilms also highlights issues of safety, delivery, and host interaction that are relevant to metabolic uses [19- 22]. Findings from biologically templated titanium nanoparticles

show that core composition and biosynthetic route strongly shape antimicrobial potency and biocompatibility principles directly relevant to choosing PEG coatings and vehicles for SPIONs [9, 22, 23]. Experience from dental nanotechnology shows that nanoparticle surface chemistry and coating critically shape mucosal compatibility, biofilm interactions, and functional performance points directly relevant to PEG-SPION dispersion and host response [24- 26]. Formulation work with iron-oxide-based systems in other indications further illustrates practical considerations for dose and vehicle selection [27]. Concurrently, artificial intelligence is accelerating nanomaterials research supporting design, screening, and optimization of nanosystems through data-driven models that shorten iteration cycles and improve translatability [28]. Regional deployments of machine learning pipelines illustrate robust feature engineering and validation workflows that can be adapted for preclinical biomarker prediction and dose-response modeling [29]. This can be applied in many fields such as parasite epidemiology [30-32], microorganisms' molecular detection [33- 35] and environment pollution [36- 40].

Despite these advances, direct head-to-head evaluations of PEG-SPIONs versus orlistat and tests of whether combining them yields additional metabolic benefit remain limited and sometimes report divergent outcomes [6, 7]. Clarifying their relative and combined effects on core metabolic readouts is therefore warranted. Here, we assess the comparative and combined

Table 1. Fasting glucose (mg/dl), serum insulin ( $\mu$ U/ml), and leptin (ng/ml) in control and obese mice after treatment with orlistat, PEG-coated superparamagnetic iron-oxide nanoparticles (SPIONs), or both.

Groups	Glucose (mg /dl)	Insulin ( $\mu$ U/ml)	Leptin (ng/ml)
A (Control)	167.428 $\pm$ 33.806 <sup>a</sup>	1.412 $\pm$ 0.483 <sup>a</sup>	42.509 $\pm$ 10.717 <sup>ac</sup>
B (Obese mice)	288.428 $\pm$ 47.243 <sup>b</sup>	1.573 $\pm$ 0.531 <sup>a</sup>	54.459 $\pm$ 16.370 <sup>ab</sup>
C (Orlistat)	264.500 $\pm$ 49.985 <sup>bc</sup>	1.263 $\pm$ 0.721 <sup>a</sup>	56.460 $\pm$ 16.463 <sup>b</sup>
D (Iron oxide)	236.071 $\pm$ 32.638 <sup>c</sup>	1.386 $\pm$ 0.576 <sup>a</sup>	33.764 $\pm$ 11.670 <sup>c</sup>
E (Orlistat + Iron oxide)	238.285 $\pm$ 26.733 <sup>c</sup>	1.476 $\pm$ 0.488 <sup>a</sup>	56.569 $\pm$ 21.655 <sup>b</sup>

a, b, c: Means within a column sharing different superscripts differ significantly ( $P < 0.05$ ).

impacts of orlistat and PEG-coated SPIONs in an obese male mouse model. We quantify fasting glucose, serum insulin, and leptin after short-term exposure to orlistat alone, PEG-SPIONs alone, or co-administration, alongside obese and non-obese controls. Our working premise was that PEG-SPIONs would match or surpass orlistat with respect to glycemic control and adipokine profile, and that co-treatment might confer additive effects. This design enables a direct appraisal of two mechanistically distinct interventions fat-absorption blockade versus nanoparticle-driven thermogenic or adipose remodeling using clinically relevant biochemical endpoints.

## MATERIALS AND METHODS

### Animal Ethics and Housing

Seventy adult male Swiss albino mice (20-25 g) were obtained from the Animal Husbandry Unit, Biology Department, College of Science, University of Misan. All procedures adhered to institutional guidelines for animal care and use. Mice were housed in standard plastic cages at 20-25 °C with a 12 h light and 12 h dark cycle and had ad libitum access to food and water. Animals were acclimatized for one week before experimental interventions.

### Induction of Obesity

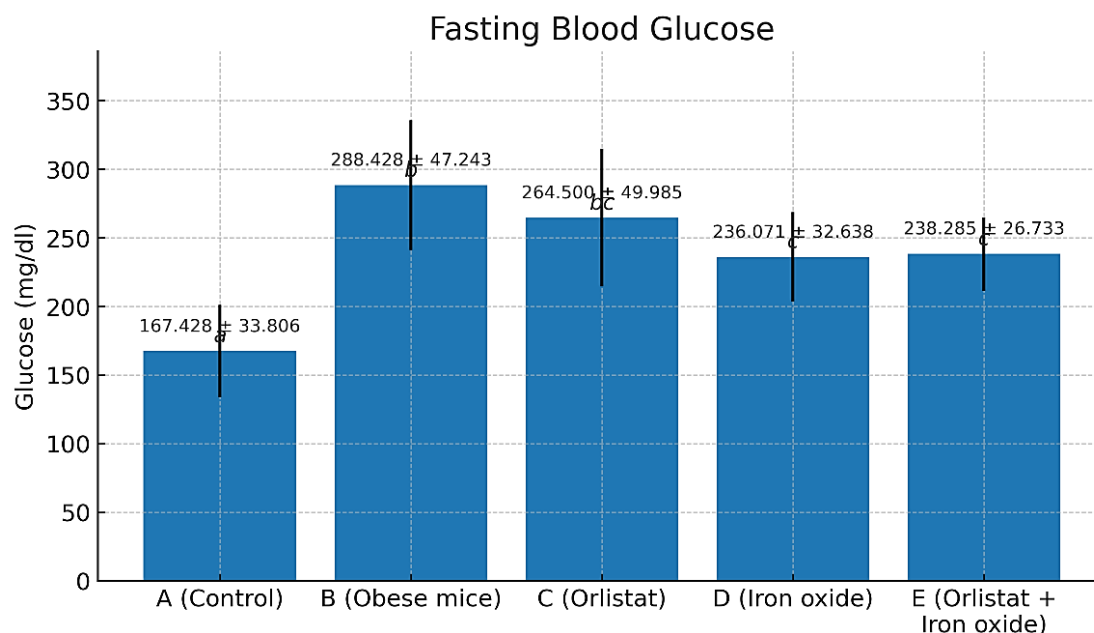
All mice, except the control group (A), were fed a high-fat diet (HFD; 60 % kcal from fat) for four weeks to induce obesity. Body weight and food intake were measured weekly. Obesity was confirmed when mice gained  $\geq 20\%$  of baseline body weight.

### Experimental Design

Once obesity was established, mice were randomly assigned (n = 14 per group) into five groups: Group A (Control): Standard diet + saline (0.2 mL/d, oral), Group B (Obese): HFD + saline (0.2 mL/d, oral), Group C (Orlistat): HFD + orlistat (120 mg/kg/d in 0.2 mL saline, oral), Group D (SPIONs): HFD + iron oxide nanoparticles ( $\text{Fe}_3\text{O}_4$ ; dose proportional to body weight, in 0.2 mL saline, oral) and Group E (Orlistat + SPIONs): HFD + orlistat (120 mg/kg/d) +  $\text{Fe}_3\text{O}_4$  SPIONs (same dose as Group D). Treatments were administered once daily for 21 days. Seven mice per group were sacrificed on day 7, and the remaining seven on day 21 for biochemical analyses.

### Reagents and dosing

Orlistat Capsules (Pharma International, Jordan) were administered at 120 mg/kg/



Different letters indicate groups that differ at  $P < 0.05$ .

Fig. 1. Fasting blood glucose across the study groups.

day in a daily oral volume of 0.2 ml. Iron-oxide nanoparticles. Fe<sub>3</sub>O<sub>4</sub> nanoparticles [PEG-coated, if applicable] were obtained from US Research Nanomaterials, Inc. Suspensions were prepared and given once daily by oral gavage at a body-weight-adjusted dose in a total volume of 0.2 ml. Combination. Group E received both agents in the same daily volume (0.2 mL), each at the doses described above.

**Blood Collection and Serum Preparation**

At each time point (days 7 and 21), mice were euthanized by chloroform inhalation. Cardiac puncture was performed using a 3 mL syringe to collect blood into gel-coated tubes. Samples were allowed to clot at room temperature for 30 min, then centrifuged at 3,000 rpm for 15 min. Serum was aliquoted into pre-labeled Eppendorf tubes and stored at -80 °C until analysis.

**Biochemical assays**

Serum glucose, insulin, and leptin were quantified. Glucose was measured. Insulin and leptin were determined by immunoassay using the Cobas e 411 analyzer (Roche, Germany).

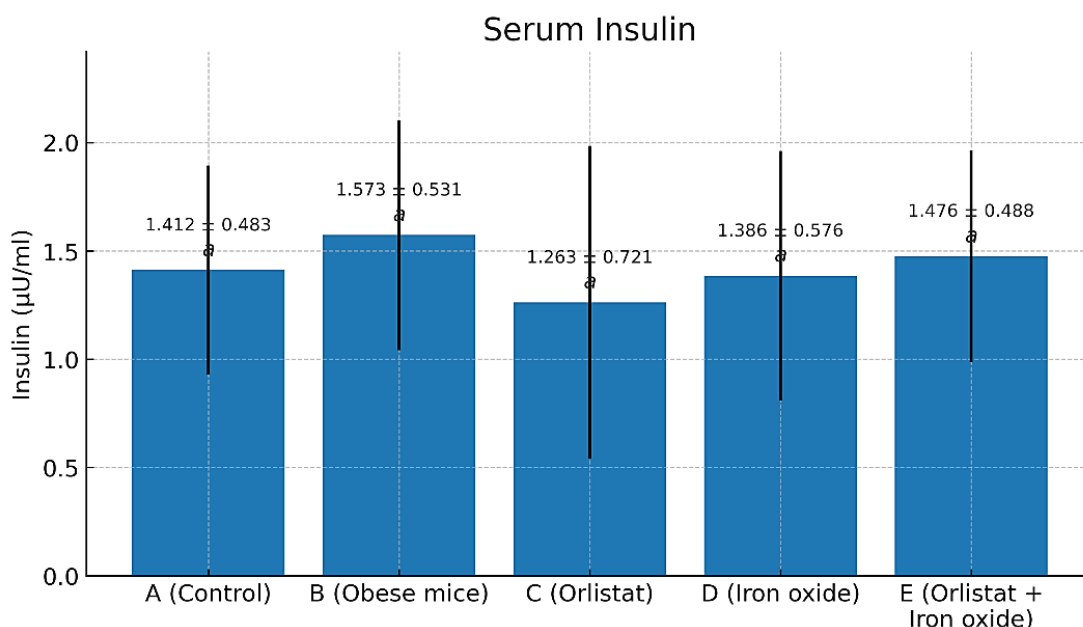
**Statistical Analysis**

Data were presented as Mean ± standard error (SE). Statistical comparisons among groups were performed using one-way analysis of variance (ANOVA), followed by Tukey’s multiple-comparisons test. A P-value < 0.05 was considered statistically significant. All analyses were conducted using SPSS version 24.0 (IBM Corp., USA).

**RESULTS AND DISCUSSION**

The effects of orlistat, PEG-coated SPIONs, and their combination on fasting glucose, serum insulin, and leptin are presented in Table 1. Data are mean ± SD for each group: A (Control), B (Obese mice), C (Orlistat), D (Iron oxide), and E (Orlistat + Iron oxide). Within each analyte, values that do not share a superscript letter are different at P < 0.05; values that share at least one letter are not different (P > 0.05).

Fasting glucose was elevated in all experimental groups relative to controls (A: 167.428 ± 33.806 mg/dl). Values were highest in obese untreated mice (B: 288.428 ± 47.243 mg/dl) and exceeded those of the iron-oxide group (D: 236.071 ± 32.638



Different letters indicate groups that differ at P < 0.05.

Fig. 2. Serum insulin levels across the study groups.

mg/dl) and the combination group (E:  $238.285 \pm 26.733$  mg/dl) ( $P < 0.05$ ). Orlistat alone (C:  $264.500 \pm 49.985$  mg/dl) did not differ from B ( $P > 0.05$ ) and was statistically comparable to D and E ( $P > 0.05$ ). Thus, B, C, D, and E were each higher than A ( $P < 0.05$ ), B was higher than D and E ( $P < 0.05$ ), and no differences were detected among C, D, and E ( $P > 0.05$ ) (Fig. 1).

Serum insulin showed no between-group differences (A:  $1.412 \pm 0.483$ ; B:  $1.573 \pm 0.531$ ; C:  $1.263 \pm 0.721$ ; D:  $1.386 \pm 0.576$ ; E:  $1.476 \pm 0.488$   $\mu$ U/ml; all  $P > 0.05$ ) as shown in Fig. 2.

Leptin concentrations were higher in the orlistat (C:  $56.460 \pm 16.463$  ng/ml) and combination (E:  $56.569 \pm 21.655$  ng/ml) groups compared with control (A:  $42.509 \pm 10.717$  ng/ml) and iron-oxide alone (D:  $33.764 \pm 11.670$  ng/ml) ( $P < 0.05$ ). Control and obese untreated mice (B:  $54.459 \pm 16.370$  ng/ml) did not differ ( $P > 0.05$ ), nor did B vs C or B vs E ( $P > 0.05$ ), and A vs D was also not different ( $P > 0.05$ ). Consistent with the grouping letters in the table (A = ac, B = ab, C = b, D = c, E = b), B exceeded D ( $P < 0.05$ ), whereas C and E were comparable to each other ( $P > 0.05$ ) as shown in Fig. 3.

In the present model, fasting glucose was higher in all experimental groups than in controls, with the greatest elevation in obese untreated mice. This pattern accords with prior reports

in obese male rodents [41]. The hyperglycemia observed in obesity is well explained by insulin resistance, in which adipose expansion increases circulating free fatty acids (FFAs), blunting insulin's anti-lipolytic action and impairing whole-body glucose disposal [1]. Obesity-associated oxidative stress further disrupts insulin signaling, reinforcing insulin resistance [2].

Despite these metabolic disturbances, insulin concentrations did not differ among groups in our study. This lack of divergence may reflect biological variability, fasting conditions at sampling, and/or limited duration of the interventions, even though the literature frequently describes hyperinsulinemia in obese models [1]. In other words, the direction of effect in the literature is consistent with insulin resistance, but our cohort did not reach statistical separation.

Administration of orlistat reduced glucose relative to obese controls only numerically (the B vs C contrast was not significant), aligning with work in rats and mice showing improvements in glycemia and insulin action [42- 44]. Mechanistically, orlistat can improve insulin sensitivity by lowering fat mass [5, 45] and mitigating oxidative stress, including through reduced LDL oxidation [46]. In our dataset, these effects were modest within the study window and did not translate into a

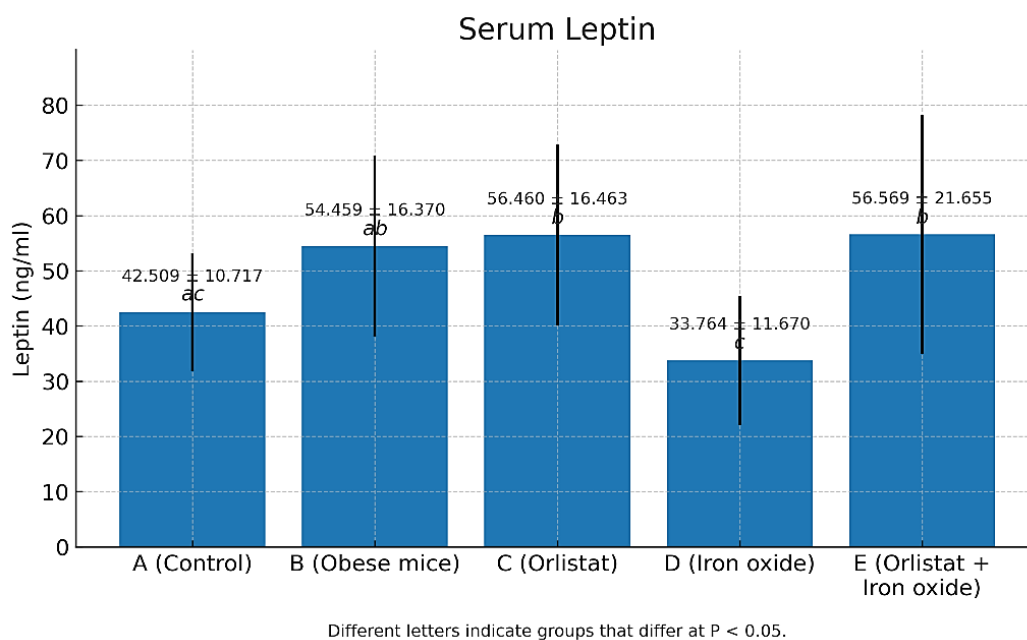


Fig. 3. Serum leptin levels across the study groups.

detectable change in insulin.

Treatment with iron-oxide nanoparticles (IONPs) yielded a clearer glycemic benefit: glucose was significantly lower than in obese mice, consistent with prior rat studies [6, 7]. Proposed mechanisms include promotion of brown adipocyte biogenesis and activity, shifting energy balance away from storage and thereby improving glucose–insulin homeostasis [47–50]. Notably, the glucose reduction with IONPs was greater than with orlistat alone in our study similar to Alsenousy et al. [7] but differing from Refaat et al. [6]. Conversely, the insulin decreases favored orlistat numerically over IONPs, paralleling Refaat et al. (2024) [6] and Alsenousy et al. (2022), [7] yet again without statistical separation in our data.

For the combination (orlistat + IONPs), we observed improved glucose relative to obese controls, but no superiority over IONPs alone. Prior work in rats reported greater improvements with the combination [6, 7]. The absence of additivity here may relate to dosing, exposure time, formulation, or route factors that can influence the pharmacodynamic overlap between fat-absorption blockade and thermogenic or browning pathways.

Regarding leptin, obese mice showed a higher mean than controls but the difference was not statistically significant in our study. The literature generally reports elevated leptin with obesity in male mice [51], a response linked to hyperinsulinemia and leptin resistance [3, 4, 52, 53]. Orlistat did not reduce leptin relative to obese controls in our cohort, which may reflect the short intervention, dose, or administration method [54, 55]. By contrast, IONPs lowered leptin compared with obese and orlistat groups, consistent with reports that IONPs suppress WAT expansion and enhance BAT activity [6, 7]. The combination failed to lower leptin versus obese controls and was higher than IONPs alone, suggesting that, under our conditions, the leptin-lowering signal from IONPs was not preserved when paired with orlistat.

## CONCLUSION

In this obesity model, none of the interventions restored fasting glycemia to control values. Nevertheless, PEG-coated superparamagnetic iron-oxide nanoparticles (IONPs) either alone or combined with orlistat lowered glucose relative to obese untreated mice, whereas

orlistat monotherapy did not. Fasting insulin was unchanged across groups, indicating that the glycemic effects observed were not accompanied by detectable shifts in basal insulin concentrations over the study period. Leptin responded divergently: IONPs alone produced lower leptin than both control and orlistat groups, while orlistat alone or with IONPs showed higher leptin than control and IONPs, and did not differ from obese animals. Taken together, these data identify IONPs as the principal driver of metabolic benefit in this design, with no clear additive advantage from co-administration with orlistat under the doses, route, and duration tested. The findings suggest that IONPs may improve glycemic control and adipokine profile through mechanisms independent of fasting insulin, whereas orlistat's expected benefits were not realized within the current regimen and may counter the leptin-lowering signal. Future studies should optimize dosing and exposure, extend treatment duration, and incorporate direct indices of insulin sensitivity (e.g., ITT/HOMA-IR), oxidative stress markers, and adipose/browning readouts to define mechanism. On present evidence, IONP monotherapy merits priority for further development, and combination therapy with orlistat should be revisited only after pharmacologic optimization. As AI tools move into biomedicine, parallel advances in healthcare cybersecurity underscore the need for rigorous data stewardship when integrating ML analytics into preclinical pipelines.

## ACKNOWLEDGMENTS

The authors thank the Animal Husbandry Unit of the Biology Department, College of Science, University of Maysan, for technical support. We also acknowledge US Research Nanomaterials, Inc. for providing the SPIONs used in this study.

## CONFLICT OF INTEREST

The authors declare that there is no conflict of interests regarding the publication of this manuscript.

## REFERENCES

1. Boden G. Obesity, insulin resistance and free fatty acids. *Current Opinion in Endocrinology, Diabetes and Obesity*. 2011;18(2):139-143.
2. Evans JL, Maddux BA, Goldfine ID. The Molecular Basis for Oxidative Stress-Induced Insulin Resistance. *Antioxidants and Redox Signaling*. 2005;7(7-8):1040-1052.
3. Lustig RH, Sen S, Soberman JE, Velasquez-Mieyer PA. Obesity, leptin resistance, and the effects of insulin reduction.

- International Journal of Obesity. 2004;28(10):1344-1348.
4. Izquierdo AG, Crujeiras AB, Casanueva FF, Carreira MC. Leptin, Obesity, and Leptin Resistance: Where Are We 25 Years Later? *Nutrients*. 2019;11(11):2704.
  5. Ke J, An Y, Cao B, Lang J, Wu N, Zhao D. Orlistat-Induced Gut Microbiota Modification in Obese Mice. *Evid Based Complement Alternat Med*. 2020;2020(1).
  6. Refaat H, Dowidar M, Ahmed A, Khamis T, Abdelhaleem S, Abdo S. The Corrective role of superparamagnetic iron oxide nanoparticles for the genes controlling hypothalamus-pituitary-testis-axis in male obesity associated secondary hypogonadism. *Open Veterinary Journal*. 2024;14(1) (Zagazig Veterinary Confer):428.
  7. Alsenousy AHA, El-Tahan RA, Ghazal NA, Piñol R, Millán A, Ali LMA, et al. The Anti-Obesity Potential of Superparamagnetic Iron Oxide Nanoparticles against High-Fat Diet-Induced Obesity in Rats: Possible Involvement of Mitochondrial Biogenesis in the Adipose Tissues. *Pharmaceutics*. 2022;14(10):2134.
  8. Al-Abboodi A, Mhouse Alsaady HA, Banoon SR, Al-Saady M. Conjugation strategies on functionalized iron oxide nanoparticles as a malaria vaccine delivery system. *Bionatura*. 2021;3(3):2009-2016.
  9. Behnia B, Aali Anvari A, Safardoust-Hojaghan H, Salavati-Niasari M. Positive effects of novel nano-zirconia on flexural and compressive strength of Portland cement paste. *Polyhedron*. 2020;177:114317.
  10. Al-Abboodi A, Tjeung R, Doran PM, Yeo LY, Friend J, Yik Chan PP. In Situ Generation of Tunable Porosity Gradients in Hydrogel-Based Scaffolds for Microfluidic Cell Culture. *Advanced Healthcare Materials*. 2014;3(10):1655-1670.
  11. Al-Abboodi A, Tjeung R, Doran P, Yeo L, Friend J, Chan P. Microfluidic chip containing porous gradient for chemotaxis study. *SPIE Proceedings*; 2011/12/21: SPIE; 2011. p. 82041H.
  12. Cheng KW, Alhasan L, Rezk AR, Al-Abboodi A, Doran PM, Yeo LY, et al. Fast three-dimensional micropatterning of PC12 cells in rapidly crosslinked hydrogel scaffolds using ultrasonic standing waves. *Biofabrication*. 2019;12(1):015013.
  13. Al-Abboodi A, Albukhaty S, Sulaiman GM, Al-Saady MAAJ, Jabir MS, Abomughaid MM. Protein Conjugated Superparamagnetic Iron Oxide Nanoparticles for Efficient Vaccine Delivery Systems. *Plasmonics*. 2023;19(1):379-388.
  14. Kim Y, Abuelfilat AY, Hoo SP, Al-Abboodi A, Liu B, Ng T, et al. Tuning the surface properties of hydrogel at the nanoscale with focused ion irradiation. *Soft Matter*. 2014;10(42):8448-8456.
  15. AlHasan L, Qi A, Al-Abboodi A, Rezk A, Shilton RR, Chan PPY, et al. Surface acoustic streaming in microfluidic system for rapid multicellular tumor spheroids generation. *SPIE Proceedings*; 2013/12/07: SPIE; 2013. p. 89235C.
  16. Kim Y, Al-Saady M, Djoulde A, Chan PPY, Shen H-H, Sengupta S, et al. Site-specific porous hydrogel coating and characterization for tunable drug- eluting ureteral stent. *Int J Pharm*. 2026;696:126807.
  17. Kim Y, Al-Saady M, Chan PPY, Shen H, Sengupta S, Fu J. Development of Site Specific Coating and Assessments for Drug-Eluting Ureteral Stents. 2024 IEEE-EMBS Conference on Biomedical Engineering and Sciences (IECBES); 2024/12/11: IEEE; 2024. p. 448-451.
  18. Dhuha NAAg, Mohammed SSALE. Spectrophotometric determination of methyl dopa by oxidative coupling reactions using 2,4 -dinitrophenylhydrazine reagent. *Tikrit Journal of Pure Science*. 2022;27(5):16-22.
  19. Jabber Al-Saady MAA, Aldujaili NH, Rabeea Banoon S, Al-Abboodi A. Antimicrobial properties of nanoparticles in biofilms. *Bionatura*. 2022;7(4):1-9.
  20. Ghani Al-Muhanna S, Ameer Al-Kraety IA, Rabeea Banoon S. Statistical Analysis of COVID-19 infections according to the gender and age in Najaf Province, Iraq. *Bionatura*. 2022;7(2):1-3.
  21. Ameer Merza Al-Ameen F, Kamil Kadhim Z, Jameel Thamir A. Review of Rotifers in Iraqi waters. *Journal of Physics: Conference Series*. 2019;1294(7):072005.
  22. Saeed ZF, Sadeek GT, Jameel RK. Synthesis and Characterization of Some Heterocyclic Compounds Derived from Schiff Base and Evaluation of Their Biological Activities. *Trends in Sciences*. 2026;23(5):11951.
  23. Aldujaili NH, Banoon SR. Antibacterial Characterization of Titanium Nanoparticles Nanosynthesized by *Streptococcus Thermophilus*. *Periódico Tchê Química*. 2020;17(34):311-320.
  24. Huang S, Gao S, Cheng L, Yu H. Remineralization Potential of Nano-Hydroxyapatite on Initial Enamel Lesions: An in vitro Study. *Caries Res*. 2011;45(5):460-468.
  25. Mushtaq E, Al-Abboodi AK. Comparative Prevalence of Oral Parasites in Orthodontic and Non-orthodontic Subjects. *Nigerian Journal of Parasitology*. 2023;44(2):446-456.
  26. Mushtaq E, Al-Abboodi AK. Molecular Evaluation of *Entamoeba gingivalis* and *Trichomonas tenax* isolated from orthodontic patients in Maysan Province, Iraq. *Nigerian Journal of Parasitology*. 2024;45(1):77-85.
  27. Zainab JM, Sahira K, Al-Abboodi AK, Alsaady HA. Enhancing Pediculicidal Activity Against *Pediculus humanus capitis* Using Iron Oxide Nanoparticle-Based Formulations of some Plant Extracts and Acetic Acid Solution. *Nigerian Journal of Parasitology*. 2024;45(2):460-469.
  28. Al-Abboodi A, Falih IQ, Al-Asadi M, Hussein BA, Al-Saady MAAJ, Abdullah TA, et al. Iron-oxide nanoparticles (SPIONs) enhance malaria vaccine antibody response. *Vaccine*. 2026;77:128353.
  29. Al-Sulami A, Al-Taee A. Potability of Drinking Water in Basra-Iraq. Tigris and Euphrates Rivers: Their Environment from Headwaters to Mouth: Springer International Publishing; 2021. p. 541-552. [http://dx.doi.org/10.1007/978-3-030-57570-0\\_23](http://dx.doi.org/10.1007/978-3-030-57570-0_23)
  30. WITHDRAWN: Sero-epidemiology of *Toxoplasma gondii* and risk factors among pregnant women in Africa. Springer Science and Business Media LLC; 2021. <http://dx.doi.org/10.21203/rs.2.18914/v2>
  31. The Infestation Study of *Oestrus ovis* L. 1761 in Sheep of Al-Amara Region, Maysan Province, South of Iraq. *Indian Journal of Forensic Medicine and Toxicology*. 2020.
  32. Sahira K, Al-Abboodi AK. Parasitological Contamination of Raw Vegetables collected from selected Local Markets in Maysan Province, South of Iraq. *Nigerian Journal of Parasitology*. 2023;44(2):464-473.
  33. Sahira K, Al-Abboodi AK. Comparative assessment of malaria diagnostic techniques updates. *Nigerian Journal of Parasitology*. 2024;45(1):164-172.
  34. Ameer Al-Kraety IA, Ghani Al-Muhanna S, Banoon SR. Molecular Exploring of Plasmid-mediated Ampc beta Lactamase Gene in Clinical Isolates of *Proteus mirabilis*. *Bionatura*. 2021;3(3):2017-2021.
  35. Baqer Al-Mayali EJ, Al-Muhanna SG, Ameer Al-Kraety IA. Detection of bla-AIM Metallo Beta Lactamase Gene among

- Stenotrophomonas Maltophilia and Carbapenem Resistant Pseudomonas Aeruginosa Isolated from Various Infections in AL- Najaf Province. *Bionatura Journal*. 2024;9(1):1-7.
36. Sofo A, Elshafie HS, Camele I. Structural and Functional Organization of the Root System: A Comparative Study on Five Plant Species. *Plants*. 2020;9(10):1338.
37. Alshahri M, Al-Mashhadany M. Evaluation of Surface Water Quality for Aquatic Life Using Artificial Intelligence Method. *Egyptian Journal of Aquatic Biology and Fisheries*. 2025;29(1):2879-2892.
38. Üstün R, Amjid M. Assessment of Germination and Seedling Development Factors of Soybean Cultivars in Different Salinity Levels. *Black Sea Journal of Agriculture*. 2024;7(5):477-485.
39. Hassan S, Al\_Ezee AMM, Al Sulivany BSA, Hassan NE. Evaluating the Ecological Consequences of Heavy Metals Contamination on Aquatic Ecosystem Functioning in the Tigris River, Iraq. *Egyptian Journal of Aquatic Biology and Fisheries*. 2026;30(2):191-202.
40. Mousa AA, Hassan SA-DH, Rashid MK, Al-Saady M. Safeguarding Patient Data: Machine Learning for Phishing URL Detection in Healthcare Systems. *Journal of Advanced Research Design*. 2025;131(1):47-60.
41. Abbas MA, Bobby N, Lee E-B, Hong J-H, Park S-C. Anti-Obesity Effects of Ecklonia cava Extract in High-Fat Diet-Induced Obese Rats. *Antioxidants*. 2022;11(2):310.
42. Review for "Anti-obesity effect of unsaponifiable matter from hemp seed in 3T3-L1 adipocytes and high-fat diet-induced obese mice". *Royal Society of Chemistry (RSC)*; 2025. <http://dx.doi.org/10.1039/d5fo02231b/v2/review2>
43. Zakaria Z, Othman ZA, Bagi Suleiman J, Jalil NAC, Ghazali WSW, Mohamed M. Protective and Therapeutic Effects of Orlistat on Metabolic Syndrome and Oxidative Stress in High-Fat Diet-Induced Metabolic Dysfunction-Associated Fatty Liver Disease (MAFLD) in Rats: Role on Nrf2 Activation. *Veterinary Sciences*. 2021;8(11):274.
44. Xu G, Zhao Z, Wysham WZ, Roque DR, Fang Z, Sun W, et al. Orlistat exerts anti-obesity and anti-tumorigenic effects in a transgenic mouse model of endometrial cancer. *Front Oncol*. 2023;13.
45. Cho LW, Kilpatrick ES, Keevil BG, Coady AM, Atkin SL. Effect of metformin, orlistat and pioglitazone treatment on mean insulin resistance and its biological variability in polycystic ovary syndrome. *Clin Endocrinol (Oxf)*. 2009;70(2):233-237.
46. Othman ZA, Zakaria Z, Suleiman JB, Ghazali WSW, Mohamed M. Anti-Atherogenic Effects of Orlistat on Obesity-Induced Vascular Oxidative Stress Rat Model. *Antioxidants*. 2021;10(2):251.
47. Maliszewska K, Kretowski A. Brown Adipose Tissue and Its Role in Insulin and Glucose Homeostasis. *Int J Mol Sci*. 2021;22(4):1530.
48. Al-Ali ZJ, Al-Saidy E. Evaluation of osteocalcin and reproductive hormones in men with type 2 diabetes in Misan province/Iraq. *Medical Journal of Babylon*. 2020;17(2):126.
49. Al-Ali ZJR, Aati E. Effect of hypothyroidism on lipid profile in women at Misan City/Iraq. *Medical Journal of Babylon*. 2020;17(1):1.
50. Li J, Cha R, Luo H, Hao W, Zhang Y, Jiang X. Nanomaterials for the theranostics of obesity. *Biomaterials*. 2019;223:119474.
51. Song J, Kim J, Park HJ, Kim H. Anti-Obesity Effects of a Prunus persica and Nelumbo nucifera Mixture in Mice Fed a High-Fat Diet. *Nutrients*. 2020;12(11):3392.
52. Madhi R, Hashim NA, Al-Ali ZAJR, Tahir NT. Estimation of lipid profile and some inflammatory biomarkers in patients with diabetes mellitus type 2 linked to hypertension. *Journal of Biological Research - Bollettino della Società Italiana di Biologia Sperimentale*. 2024.
53. Abed Aldraji RA, Abdul Jabbar Ridha Al-Ali Z. Effect of hydroxychloroquine and Artemisia herba-alba administration on liver enzymes and kidney functions in laboratory male mice. *Egyptian Journal of Chemistry*. 2022;0(0):0-0.
54. Caroline OB, Ebuehi OAT, Cecilia OA, Kayode OA. Effect of Allium sativum extract in combination -with orlistat on insulin resistance and disrupted metabolic hormones in high fat diet induced obese rats. *Scientific African*. 2021;14:e00994.
55. Yilmaz A, Toraman MN, Mataraci Karakas S, Ozden Z, Pinarbas E, Mercantepe T. Effect of White Tea on Leptin and Asprosin Levels in Rats Feeding a High-Fat Diet. *Life*. 2024;14(12):1548.